Arctic Tropospheric Ozone Trends

K. S. Law[1], J. Liengaard Hjorth[2], J. B. Pernov[2,3], C. H. Whaley[4], H. Skov[2], M. Collaud Coen[5], J. Langner[6], S. R. Arnold[7], D. Tarasick[8], J. Christensen[2], M. Deushi[9], P. Effertz[10,14], G. Faluvegi[11,12], M. Gauss[13], U. Im[2], N. Oshima[9], I. Petropavlovskikh[10,14], D. Plummer[4], K. Tsigaridis[11,12], S. Tsyro[13], S. Solberg[15] and S.T. Turnock[16,7]

[1]Sorbonne Université, LATMOS-IPSL, UVSQ, CNRS, Paris, France
[2]Department of Environmental Science, Interdisciplinary Centre for Climate Change, Aarhus University, Frederiksborgvej 4000, Roskilde, Denmark
[3]Extreme Environments Research Laboratory, École Polytechnique Fédérale de Lausanne, 1951 Sion, Switzerland
[4]Canadian Centre for Climate modeling and analysis, Environment and Climate Change Canada, Victoria, BC, Canada
[5]Federal Office of Meteorology and Climatology, MeteoSwiss, Payerne, Switzerland
[6]Swedish Meteorological and Hydrological Institute, Norrköping, Sweden
[7]Institute for Climate and Atmospheric Science, School of Earth and Environment, University of Leeds, Leeds, United Kingdom
[8]Air Quality Research Division, Environment and Climate Change Canada, Toronto, ON, Canada
[9]Meteorological Research Institute, Japan Meteorological Agency, Tsukuba, Japan
[10]Cooperative Institute for Research in Environmental Sciences (CIRES), University of Colorado, Boulder, CO, USA.
[11]NASA Goddard Institute for Space Studies, New York, NY, USA
[12]Center for Climate Systems Research, Columbia University; New York, USA
[13]Norwegian Meteorological Institute, Oslo, Norway
[14]National Oceanic and Atmospheric Administration (NOAA) ESRL Global Monitoring Laboratory, Boulder, CO, USA.
[15]Norwegian Institute for Air Research (NILU), Kjeller, Norway.
[16]Met Office Hadley Centre, Exeter, UK

Corresponding author: Kathy.Law@latmos.ipsl.fr

Key Points:

- Coherent ozone trend analysis methodology applied to multi-decade, pan-Arctic surface and ozonesonde datasets and multi-model medians.
- Increasing winter Arctic tropospheric ozone overestimated by models in the free troposphere, Alaskan spring surface increases not captured.
- Spring (summer) decreases (increases) in observed ozone throughout the troposphere, not always simulated by models.

Abstract

Trends in tropospheric ozone, an important air pollutant and short-lived climate forcer (SLCF), are estimated using available surface and ozonesonde profile data for 1993-2019. Using a coherent methodology, observed trends are compared to modeled trends (1995-2015) from the Arctic Monitoring Assessment Programme SLCF 2021 assessment. Statistically significant increases in observed surface ozone at Arctic coastal sites, notably during winter, and concurrent decreasing trends in surface carbon monoxide, are generally captured by multi-model median (MMM) trends. Wintertime increases are also estimated in the free troposphere at most Arctic sites, but tend to be overestimated by the MMMs. Springtime surface ozone increases in northern coastal Alaska are not simulated while negative springtime trends in northern Scandinavia are not always reproduced. Possible reasons for observed changes and model behavior are discussed, including decreasing precursor emissions, changing ozone sinks, and variability in large-scale meteorology.

Plain Language Summary

The Arctic is warming much faster than the rest of the globe due to increases in carbon dioxide, and other trace constituents like ozone, also an air pollutant. However, improved understanding is needed about long-term changes or trends in Arctic tropospheric ozone. A coherent methodology is applied to determine trends in surface and regular profile measurements over the last 20-30 years, and results from six chemistry-climate models. Statistically significant increases in observed ozone are found at the surface and in the free troposphere during winter in the high Arctic. Paradoxically, decreases in nitrogen oxide emissions at mid-latitudes appear to be leading to increases in ozone during winter, but associated increases in Arctic tropospheric ozone tend to be overestimated in the models. Increases are also found at the surface in northern Alaska during spring but not reproduced by the models. The causes are unknown but could be related to changes in local sources or sinks of Arctic ozone or in large-scale weather patterns. Declining mid-latitude emissions may also explain negative surface ozone trends over northern Scandinavia in spring that are not always captured by the models. Further work is needed to understand changes in Arctic tropospheric ozone.

1 Introduction

Tropospheric ozone (O_3) is a short-lived climate forcer (SLCF) contributing to global and Arctic warming (AMAP, 2015; Sand et al, 2016; von Salzen et al. 2022), and a critical secondary air pollutant, detrimental to human health (Anenberg et al., 2010) and ecosystems (Arnold et al., 2018). The Arctic tropospheric O_3 budget is complex, as recently discussed in a companion paper, Whaley et al. (2023). It originates from photochemical production of anthropogenic or

natural emissions of O_3 precursors, including nitrogen oxides (NO_x), carbon monoxide (CO) and methane (CH_4), in the Arctic, or following air mass transport from mid-latitudes, as well as transport of O_3 from the stratosphere (Law et al., 2014; Schmale et al., 2018). Sinks include photochemical destruction, including reactions involving halogens leading to so-called ozone depletion events (ODEs) (Barrie, et al., 1988; Simpson et al., 2007), and surface dry deposition (Clifton et al., 2020). Growth in anthropogenic emissions since pre-industrial times has led to increases in tropospheric O_3 throughout the Northern Hemisphere (NH) (Tarasick et al., 2019; Turnock et al., 2020; Cooper et al., 2020) contributing to observed global and Arctic warming over the past century (e.g. Griffiths et al., 2021). Since the mid-1990s, a mix of relatively weak positive and negative trends (+1 to -1 parts per billion by volume (ppbv) per decade) have been reported in the NH at the surface and in the free troposphere (FT), with largest increases over south and eastern Asia, associated with increasing anthropogenic emissions (Cooper et al., 2020; Wang et al., 2022a).

To date, only a few studies have focused on assessing tropospheric O_3 trends in the Arctic. While positive O_3 trends were diagnosed at several surface sites, results are not always statistically significant, and both positive and negative trends were reported at some Canadian sites (Tarasick et al., 2016; Sharma et al., 2019; Cooper et al., 2020). In the Arctic FT, studies found significant positive trends (Christiansen et al., 2017; Wang et al., 2022a), no trends (Tarasick et al., 2016), or mixed trends in different seasons (Bahramvash Shams et al., 2019). Differences in the periods analyzed, sign or magnitude of trends emphasizes the need to further examine trends using the same methodology. Coherent estimation of observed trends, and evaluation of modeled trends, is needed to better understand O_3 changes and impacts on Arctic climate that are sensitive to the altitude where O_3 perturbations occur (Rap et al., 2015). This study assesses annual and monthly trends, together with possible evolution in seasonal cycles, of Arctic tropospheric O_3 over the last 20-30 years. Observed changes are compared to results from atmospheric chemistry-climate models run as part of the recent Arctic Monitoring and Assessment Programme (AMAP) SLCF assessment (AMAP, 2021; Whaley et al., 2022; von Salzen et al., 2022). Results are discussed in light of possible changes in sources and sinks of Arctic tropospheric O_3.

2 Methods

2.1 Measurements

The location of surface and ozonesonde sites used in this study are displayed in Fig. 1, together with the Arctic Circle at 66.6°N, used to define the Arctic. Annual surface trends are shown in the table grouped into 1) high Arctic coastal sites (Alert, Utqiaġvik/Barrow, Villum), Zeppelin (situated at 474m on Svalbard) and Summit (high altitude (FT) site on Greenland (3211m), and 2) European continental sites within (Pallas, Esrange), and just south (Tustervatn) of the Arctic Circle.

Site	Annual trend (%)	Significance level	Period
High Arctic:			
Alert	**0.29**	95%	1999-2019
	0.24	95%	1993-2019
Utqiagvik	0.53	<90%	1999-2019
	0.26	<90%	1993-2019
Villum	**1.98**	95%	1999-2019
	0.68	90%	1996-2019
Zeppelin	-0.19	<90%	1999-2019
	0.18	90%	1993-2019
Summit	-0.28	<90%	2001-2019
European continental Arctic and near-Arctic:			
Esrange	0.08	<90%	1999-2019
	0.00	<90%	1993-2019
Pallas	**-0.30**	90%	1998-2019
	-0.40	90%	1995-2019
Tustervatn	**-0.52**	99%	1999-2019
	-0.18	>90%	1994-2019

Figure 1. *Left: Location of surface (bold) and ozonesonde (italic) sites and showing the Arctic Circle (66.55°N). Right: annual O_3 trends at surface sites in % per year (left column), the significance level (middle column), calculated over periods shown in the right column. Statistically significant trends (above 90% confidence level) are in bold. Geographical coordinates for all sites are provided in Whaley et al. (2023). See text for details.*

Surface observations are from EBAS Level 2 data, station owners for Villum before 2001, Canada's Open Government Portal for Alert, and National Oceanic and Atmospheric

Administration (NOAA) for Summit, and Barrow Atmospheric Observatory, Utqiaġvik (Utqiaġvik from now on). Ozonesonde data are from the World Ozone and Ultraviolet Radiation Data Centre (WOUDC) and Network for the Detection of Atmospheric Composition Change (NDACC). See also the Supplementary Information (Text S1, Figs. S1 and S2, including data coverage).

2.2 Trend analysis

Observed monthly and annual trends in surface O_3 concentrations at different sites are determined using the non-parametric Mann-Kendall test at the 90^{th} and 95^{th} confidence level (CL) and Sen's slope methodology (Theil, 1950; Sen, 1968) (see Text S2). Daily median data are sorted into different months and pre-whitened, due to the presence of autocorrelation, via the 3PW algorithm from Collaud Coen et al. (2020). Trends using ozonesonde profiles are calculated based on weekly medians for selected pressure levels. For the calculation of relative trends, data are normalized by division with median values and multiplied by 100.

2.3 Modeled trends

Modeled trends at the surface and different altitudes are calculated for 1995-2015 using results from four global chemistry-climate models (CMAM, GISS-E2.1, MRI-ESM2, UKESM1) and two chemistry-transport models (DEHM, EMEP MSC-W) run using the same ECLIPSEv6b anthropogenic emissions, and nudged with meteorological reanalyses as part of AMAP (2021). Details can be found in Whaley et al. (2022), Text S3 and Table S1. Simulated monthly mean O_3 volume mixing ratios from the model grid box containing the measurement location are used to compute multi-model medians (MMMs). For ozonesonde comparisons, modeled vertical profiles are interpolated onto the same vertical bins as the measurements before trends are computed.

3 Surface ozone trends in the Arctic

3.1 Observed ozone trends

Annual trends are calculated for 1993-2019, or for the longest period with sufficient data, for all the sites (see Fig. 1, Table S2).

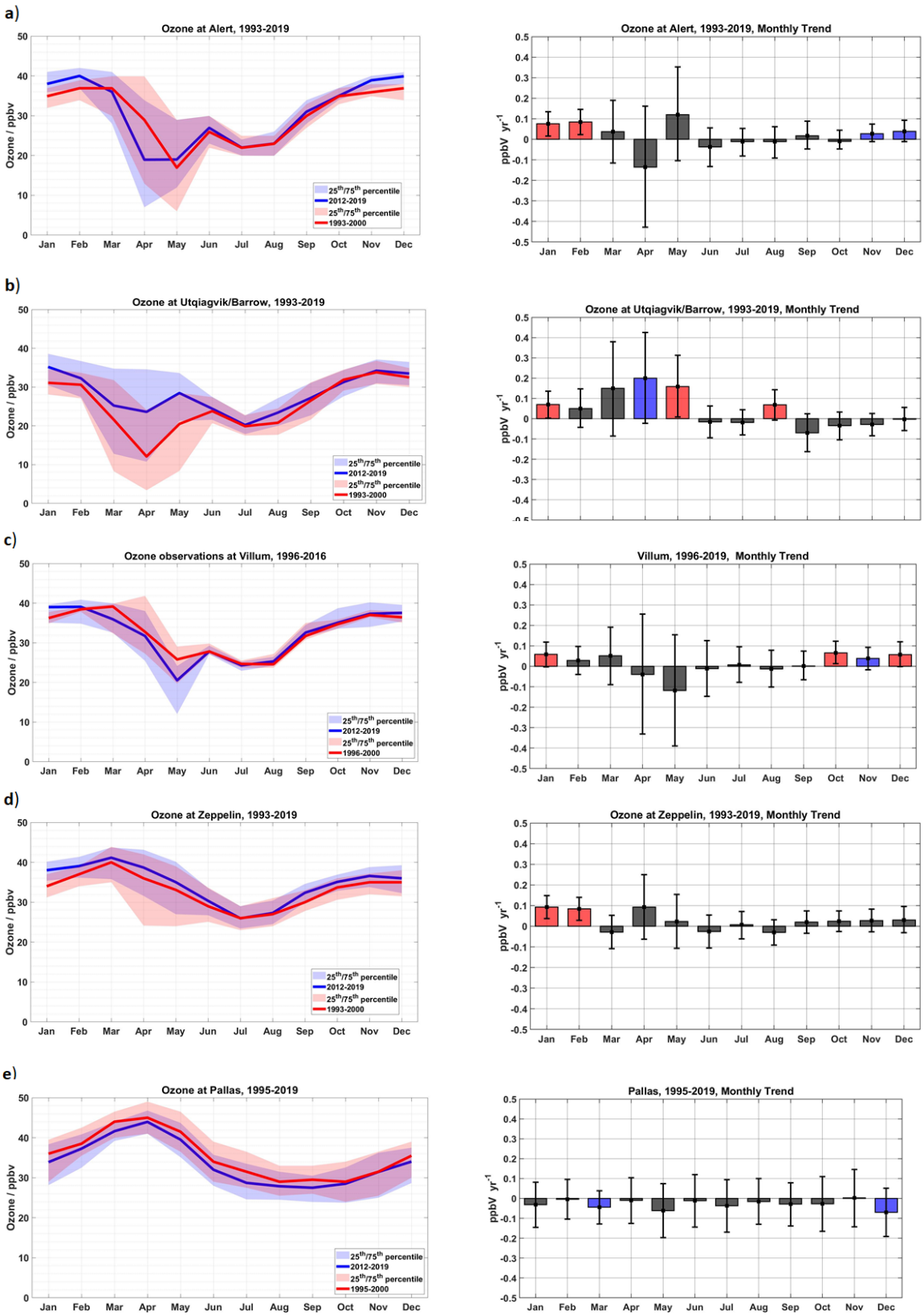
a)
Ozone at Alert, 1993-2019
Ozone / ppbv
25th/75th percentile
2012-2019
25th/75th percentile
1993-2000
Ozone at Alert, 1993-2019, Monthly Trend
ppbV yr-1
b)
Ozone at Utqiagvik/Barrow, 1993-2019
Ozone / ppbv
25th/75th percentile
2012-2019
25th/75th percentile
1993-2000
Ozone at Utqiagvik/Barrow, 1993-2019, Monthly Trend
ppbV yr-1
c)
Ozone observations at Villum, 1996-2016
Ozone / ppbv
25th/75th percentile
2012-2019
25th/75th percentile
1996-2000
Villum, 1996-2019, Monthly Trend
ppbV yr-1
d)
Ozone at Zeppelin, 1993-2019
Ozone / ppbv
25th/75th percentile
2012-2019
25th/75th percentile
1993-2000
Ozone at Zeppelin, 1993-2019, Monthly Trend
ppbV yr-1
e)
Ozone at Pallas, 1995-2019
Ozone / ppbv
25th/75th percentile
2012-2019
25th/75th percentile
1995-2000
Pallas, 1995-2019, Monthly Trend
ppbV yr-1
Jan Feb Mar Apr May Jun Jul Aug Sep Oct Nov Dec

Figure 2. *Observed surface O_3 trends and seasonal cycles. Left: seasonal cycles of monthly median O_3 (ppbv) at a) Alert, b) Utqiaġvik, c) Villum, d) Zeppelin, and e) Pallas for 1993-2000 (blue lines) vs 2012-2019 (red lines). Shaded areas show upper and lower quartiles of hourly values. Right: monthly trends for 1993-2019. Boxes represent the slope of the trend in ppbv per year with red boxes significant at 95th% CL, blue boxes at 90th% CL, and black boxes not statistically significant. Error bars show 95th% CLs. Results are shown for shorter periods depending on data availability.*

Average O_3 seasonal cycles are also calculated for earlier (1993-2000) and later (2012-2019) periods, to examine possible changes, together with monthly trends (Fig. 2) at selected sites (see Fig. S3 for other sites). Monthly trends are also analyzed for different 21-year periods (1993-2012, 1999-2019) (Fig. S4).

First considering high Arctic sites at coastal locations that exhibit a winter maximum with low spring concentrations attributed to ODEs, as discussed in Whaley et al. (2023). Alert has statistically significant ("ss") positive O_3 annual trends, as does Villum for the shorter time period 1999-2019, while annual trends at Utqiaġvik are not significant (see Fig. 1). Ss trends are also calculated in particular seasons, as shown in Fig. 2. Notably, ss positive trends are found during late autumn and/or winter at Alert, Villum and Utqiaġvik. Positive trends are also calculated for spring at Utqiaġvik (April-May). Winter trends at Alert and spring trends at Utqiaġvik are more pronounced when using the later record (1999-2019) (see Fig. S4). To further characterize these changes, probability distributions in observed O_3 concentrations are calculated for months with ss trends (see Fig. S5). Positive ss trends during winter and spring at Utqiaġvik are the result of a decrease (increase) in the frequency of low (high) concentrations (Jan.-May), whereas wintertime O_3 concentrations shifted recently towards higher values at Alert (Nov.-Feb.) and Villum (Oct.-Jan.). Zeppelin shows a different seasonal behavior compared to Arctic sea-level coastal sites with a spring maximum, more similar to remote mid-latitude sites. Here, ss positive annual trends are estimated for 1993-2019 (Fig. 1), and in winter (Fig. 2), driven by increases in the earlier part of the record (1993-2013) (Fig. S4).

Continental northern Scandinavian sites exhibit a different behavior with Pallas and Tustervatn showing ss negative annual trends but no ss annual (or monthly) trends at Esrange over any of the periods considered. The shape of the seasonal cycle for the earlier versus the later period is

similar at these sites, which also have a spring maximum like Zeppelin. O_3 appears to be decreasing throughout the year when comparing earlier and later periods although ss negative trends are only evident at Pallas (March, December), and at Tustervatn in spring and early summer (Fig. S4, 1999-2019 trends). Summit is more representative of the FT and samples air masses transported from North America and Asia, or of stratospheric origin (Dibb, 2007; Schmeisser et al., 2018). The annual trend, calculated over the shorter 2001-2019 record, is not ss at the 90th % CL, but ss negative monthly trends are estimated for January, March-May and September.

3.2 Comparison of observed and modeled surface trends

Figure 3 compares observed monthly and MMM trends for 1995-2015, or the closest possible time interval in case of years with missing observations. Results for other sites are shown in Fig. S6. Observed ss trends are more frequently diagnosed over 1993-2019 (Fig. 2) than over the shorter period ending in 2015 (Fig. 3). While the MMMs simulate O_3 seasonal cycles reasonably well, low O_3 concentrations are missed in spring, and wintertime O_3 is underestimated (Whaley et al., 2023). The MMMs simulate ss positive and negative trends at Zeppelin (Jan.) and Esrange (May), respectively, but not ss positive trends at Utqiaġvik (April). Ss trends are simulated, but not observed, at Alert (January, December) and Tustervatn (March).

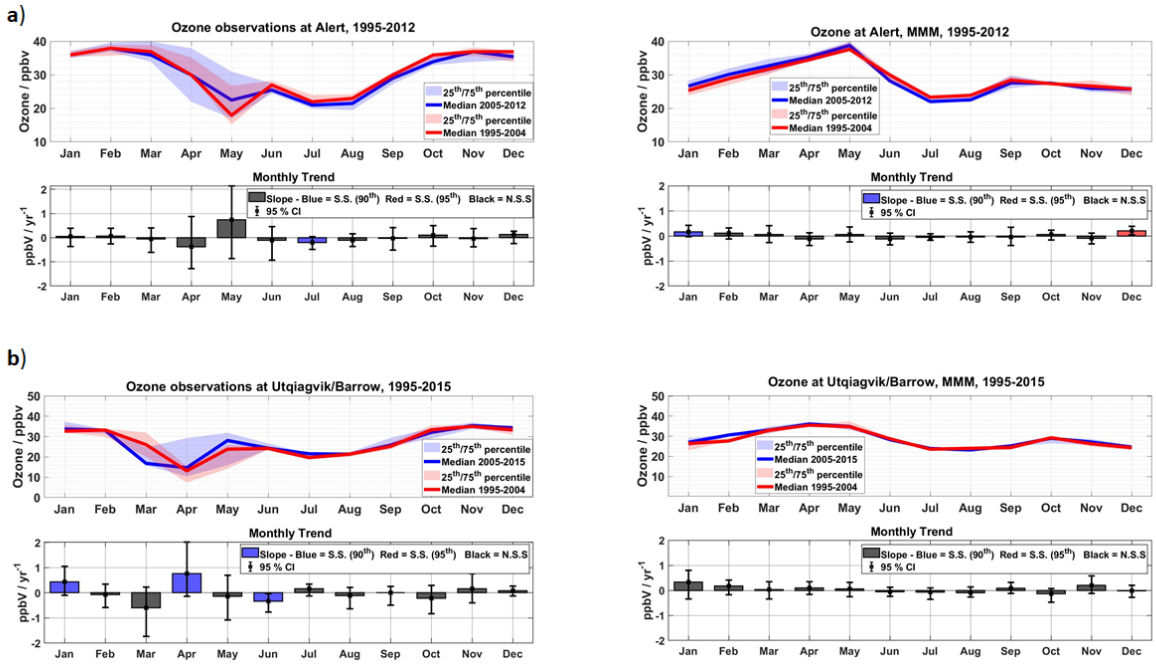

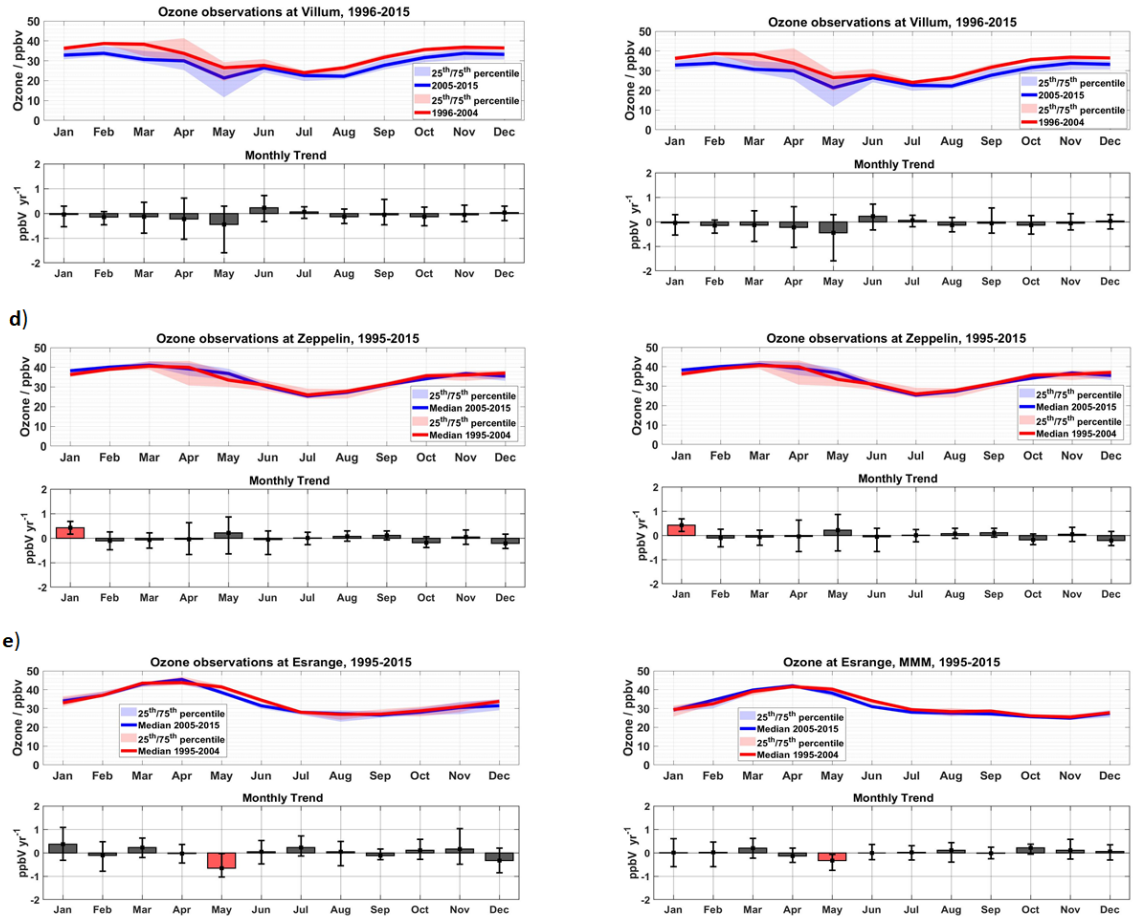

Figure 3: *Comparison of observed (left) and MMM (right) surface O_3 trends and seasonal cycles at a) Alert, b) Utqiaġvik,* c) *Villum, d) Zeppelin, and e) Esrange. Upper panels: seasonal cycles for 1995-2004 (red lines) vs 2005-2015 (blue lines). Shaded areas show upper and lower quartiles of monthly values (observations only). Lower panels: monthly median trends in ppbv per year for 1995-2015, or shorter periods depending on data availability. Box coloring and error bars are the same as Fig. 2.*

4 Arctic ozone trends in the free troposphere

4.1 Observed vertical trends

This analysis focuses on O_3 changes in the lower and mid-troposphere. Figure 4 shows observed relative trends at six Arctic ozonesonde sites from 925-400 hPa for 1993-2019. Absolute trends above and below 400 hPa, and relative trends from 925-100 hPa, are also calculated (Figs. S7a,

S7b). Overall, while there are few ss trends, there seems to be a "dipole effect" with positive trends in winter and summer, and negative trends in spring and autumn. Positive ss winter (Jan/Dec) trends are found up to 400 hPa at most sites (except Resolute), and also at Scoresbysund in early spring. Positive wintertime trends are more evident in the earlier period in the upper troposphere (UT) and lower stratosphere (LS) (Fig. S8). Eureka, Resolute, and Sodankyla have periods with negative trends especially during spring and early summer in the lower troposphere. Resolute decreases extend up to 500 hPa in March-April. Relative ss trends vary from -1.5% to +0.5-1.0 % per year (Figs. 4, S7b) while stronger negative trends are diagnosed in later years (1999-2019) compared to 1993-2013 at all sites (Fig. S8).

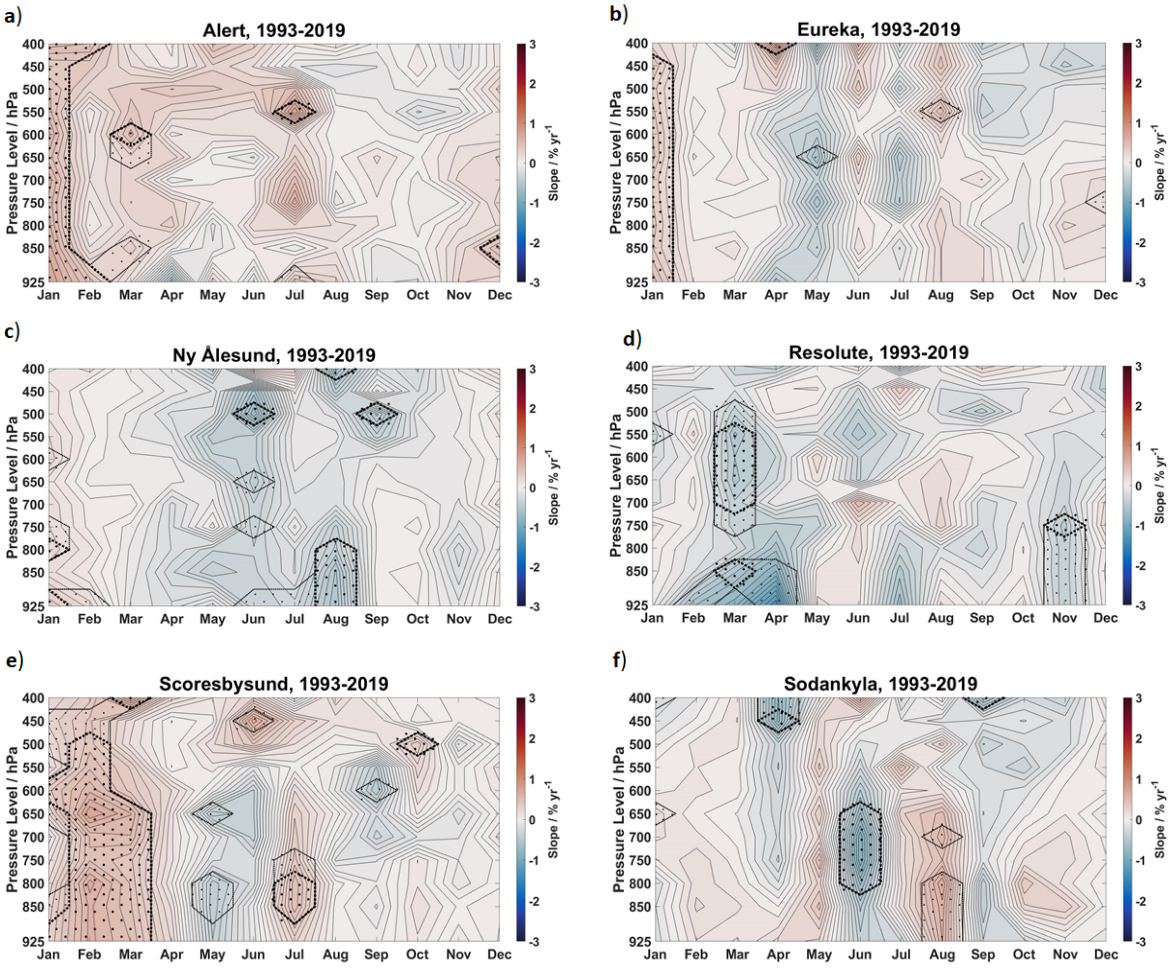

Figure 4: *Vertical trends in observed monthly O_3 for 1993-2019, relative to monthly median concentrations, in % per year, from 925-400 hPa at a) Alert, b) Eureka, c) Ny Alesund, d) Resolute, e) Scoresbysund, and f) Sodankyla. Stippled lines/areas show statistical significance at the 90th % CL (smaller marker size) and 95th % CL (larger marker size).*

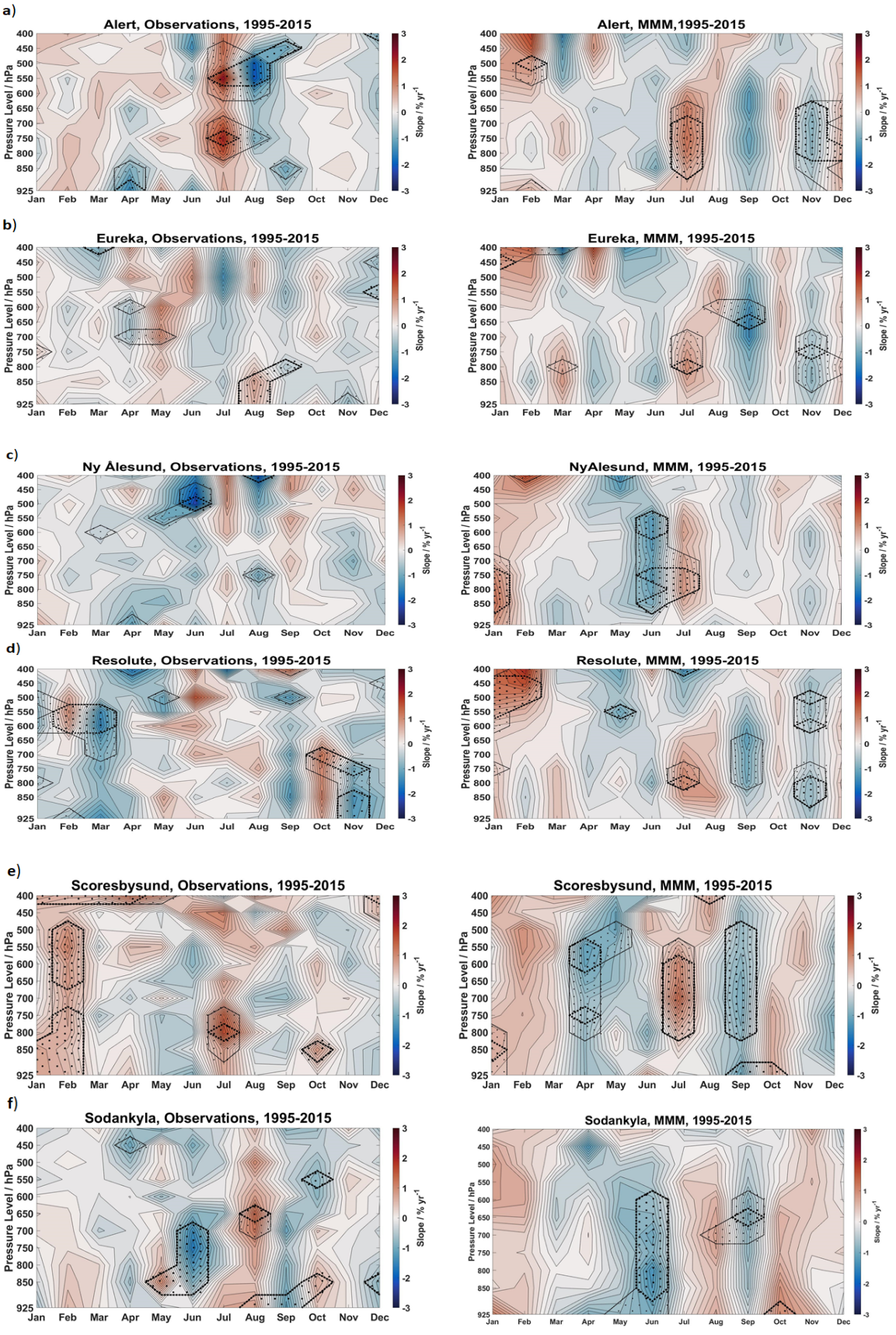
a)
Alert, Observations, 1995-2015
Alert, MMM,1995-2015
b)
Eureka, Observations, 1995-2015
Eureka, MMM, 1995-2015
c)
Ny Ålesund, Observations, 1995-2015
NyAlesund, MMM, 1995-2015
d)
Resolute, Observations, 1995-2015
Resolute, MMM, 1995-2015
e)
Scoresbysund, Observations, 1995-2015
Scoresbysund, MMM, 1995-2015
f)
Sodankyla, Observations, 1995-2015
Sodankyla, MMM, 1995-2015
Pressure Level / hPa
Slope / % yr-1
Jan Feb Mar Apr May Jun Jul Aug Sep Oct Nov Dec

Figure 5: *Comparison of observed (left) and MMM (right) vertical trends in monthly O_3, relative to monthly medians, in % per year, from 925-400 hPa over 1995-2015 at a) Alert, b) Eureka, c) Ny Alesund, d) Resolute, e) Scoresbysund, and f) Sodankyla. Shading/symbols are as in Fig. 4.*

4.2 Comparison of observed and modeled vertical trends

Figure 5 shows observed ozonesonde and MMM trends for 1995-2015 up to 400 hPa (see Fig. S9 for results up to 100 hPa). Only results from 5 models are used, since EMEP MSC-W only provided surface O_3. The MMMs appear to capture the observed "dipole effect" seen in the observed trends. Models also capture observed increases in the winter but trends are overestimated at most sites, especially Ny Alesund and Sodankyla. Negative winter trends at Resolute are not simulated. This may be linked to positive modeled trends above 500 hPa at all sites (Fig. S9). Summertime positive ss MMM trends are larger than observed trends at some sites, e.g. Resolute and Ny Alesund.

5 Discussion and conclusions

Increasing annual surface O_3 trends at Arctic coastal sites, and at Zeppelin, are in qualitative agreement with Cooper et al. (2020), but in contrast to negative or non-significant surface trends at Canadian ozonesonde sites (Tarasick et al., 2016). A notable finding is that ss positive trends occur mainly in the winter months. While such increases were reported previously at Utqiaġvik (Gaudel et al. 2018; Christiansen et al., 2022) and Alert (Sharma et al., 2019), we confirm this tendency over the wider Arctic. Emission reductions of NO_x in Europe and North America, and more recently over eastern Asia, have led to increasing wintertime O_3 at mid-latitudes due to less NO titration of O_3 (Jhun et al., 2015, Wang et al., 2022b, Bowman et al., 2022). This can explain observed increases in wintertime surface Arctic O_3, influenced primarily by transport of air masses from Europe (Hirdman et al., 2010). Evidence for declining O_3 precursor trends is supported by decreases in observed CO in the Arctic during autumn and winter (Fig. S10). At the same time, CH_4 continues to increase globally contributing to rising O_3 in the NH (Zeng et al., 2022) (see also Text S4 on Arctic O_3 precursor trends).

Another intriguing finding is springtime ss surface O_3 increases at Utqiaġvik (especially over 1999-2019, Fig S4), but no ss changes at Alert and Villum. Changes in O_3 concentrations at this

time of year may be driven by changes in ODE frequency linked to climate change or weather patterns (Oltmans et al, 2012). ODEs lead to zero or very low springtime O_3 due to bromine released from frost flowers or blowing snow (on sea-ice) (Simpson et al., 2007) or iodine compounds with a possible oceanic source (Benevant et al., 2022). Increases in springtime tropospheric bromine oxide have been observed from satellites, especially along the north coast of Greenland and central Arctic Ocean, correlating weakly with an increasing frequency in first year sea-ice (Bougoudis et al., 2020). Indeed, the frequency of low springtime O_3 concentrations has been increasing at Canadian high Arctic sites (see Fig. S11) but no ss springtime monthly trends are determined at Alert or Villum in our analysis. Springtime increases at Utqiaġvik could be due to stronger transport from mid-latitudes to this site during periods with a more northerly extension of the Pacific storm track, hampering conditions for ODEs (Koo et al., 2012). They could also be due to an increasing influence from local emissions, such as shipping or Alaskan petroleum extraction, when photochemistry becomes active in spring (Gunsch et al., 2017).

Decreases in springtime/early summer O_3 in northern Scandinavia, especially over the later 1999-2019 period, are consistent with negative trends reported at Tustervatn (Cooper et al., 2020), and sites in northern Sweden during summer (Andersson et al., 2017). These decreases are associated with lower maximum O_3 concentrations linked to reductions in European precursor emissions leading to less photochemical O_3 production (Cooper et al., 2020) although no ss trends in observed Arctic CO are found at this time of year (Fig. S10). Springtime ss negative trends at Summit may also be due to emission reductions over North America. Our results do not suggest a shift in the O_3 seasonal cycle toward higher concentrations in the spring (i.e. moving back toward pre-industrial O_3 seasonality) as reported at NH mid-latitudes (Bowman et al., 2022). Another explanation for decreasing springtime O_3 at the surface could be that reductions in snow cover (Mudryk et al., 2020) are leading to more O_3 dry deposition to Scandinavian forests.

The observed and modeled surface trend comparison covers 1995-2015, thereby missing the later time period when stronger observed O_3 trends are found, especially ss positive trends in winter. MMMs capture wintertime O_3 increases at Zeppelin, but overestimate at Alert and miss increase at Utqiaġvik. However, Whaley et al. (2023) noted that these models underestimate wintertime Arctic O_3 due to deficiencies modeling shallow boundary layers, O_3 deposition or NO_x lifetimes.

Nevertheless, decreasing winter trends in surface CO are captured at Alert and Utqiaġvik (Fig. S10). Ss positive spring O_3 trend at Utqiaġvik is not evident in MMM trends over 1995-2015. However, the models do not capture springtime O_3 seasonality due to incorrect simulation of transport patterns (Oltmans et al., 2012) or missing surface halogen chemistry (Whaley et al., 2023). Negative ss springtime (May) trends are not always reproduced, possibly reflecting issues in the emission trends or modeled dry deposition.

FT O_3 trends are ss positive in winter at all Arctic sites, except Resolute, in common with several coastal Arctic surface sites. These results are in-line with increases reported at NH mid-latitudes (Cooper et al., 2020), and at Canadian ozonesonde sites (up to 400 hPa), except Resolute (Wang et al., 2022a). MMM trends are similar to observed trends over 1995-2015, including where they are ss. Patterns in observed trends are quite well captured, notably positive ss trends in winter and summer, although they tend to be overestimated. Observed negative trends in spring, extending from near the surface into the FT, are generally reproduced, and are likely to be due to decreasing NO_x emissions leading to lower FT O_3 where photochemical production is NO_x-limited. Overestimation of winter trends contrasts to previous studies where models underestimated NH trends (Wang et al., 2022a; Christiansen et al., 2022). This may be due to differences in model transport or O_3 precursor emission trends, including NO_x reductions (see also Text S4). AMAP models overestimate mid-latitude FT O_3 (Whaley et al., 2023), possibly suggesting a larger sensitivity to precursor emission changes.

Observed trends in the UT (LS) appear to have switched from positive to negative since 1993 in winter/spring, which may explain stronger positive FT trends in the earlier part of the record (1993-2013). More frequent positive phases of the Arctic Oscillation in recent years may be contributing with a weaker Brewer-Dobson circulation leading to less transport of stratospheric O_3 into the Arctic UT-LS, a higher tropopause height, and thus lower O_3 concentrations in this region (Zhang et al., 2017). However, Liu et al. (2020) did not detect any trend in the stratospheric O_3 flux into the Arctic UT. On the other hand, Wang et al. (2022a) attributed FT increases in NH mid-high latitude O_3 to increases in aircraft NO_x emissions.

Overall, this study finds significant robust trends in Arctic tropospheric O_3. Observed trends are generally quite well captured by multi-model median results, although for example, they

overestimate wintertime free tropospheric increases, and miss Alaskan surface increases in spring. Further investigation into the causes of observed trends, and model performance, are needed taking into account uncertainties in the observations and models (Young et al., 2018; Fiore et al., 2022).

Acknowledgements

We thank colleagues involved in AMAP (2021), notably K. von Salzen (Env. Canada), M. Flanner (U. Michigan). Technicians and logistical support staff are gratefully acknowledged for their work on data collection: D. Worthy (Alert), K. Sjöberg (Esrange), K. Saarnio (Pallas), B. Jensen, C. Christoffersen, K. Mortensen (Villum), and B. Thomas (Utqiaġvik/Barrow). None of the authors declare any real or perceived financial conflicts of interests. Multiple funders are acknowledged for support (see author metadata).

Data Availability Statement:

Surface O_3 monitoring datasets are provided by EMEP (European Monitoring and Evaluation Program), and Global Atmosphere Watch (GAW) World Data Centre for Reactive Gases. EMEP and GAW O_3 data are available via the EBAS data portal (from end of 1989 to present). CO data at Utqiaġvik/Barrow and Zeppelin are also available via the EBAS data portal: http://ebas.nilu.no. Select the station name, and the component (CO, O_3) to access the data files. Canadian surface O_3 data can be downloaded from: https://data-donnees.ec.gc.ca/data/air/monitor/networks-and-studies/alert-nunavut-ground-level-ozone-study/. Canadian surface CO is available at: https://data-donnees.ec.gc.ca/data/air/monitor/national-air-pollution-surveillance-naps-program/?lang=en. Click on folders Data, Year, ContinuousData, then HourlyData. Surface O_3 records for Utqiaġvik/Barrow (BRW) and Summit (SUM) are provided by PE and IE via NOAA GML. Data is available at https://gml.noaa.gov/aftp/data/ozwv/SurfaceOzone/. Click on the directories for BRM or SUM to obtain the data. Surface O_3 measurements at Summit are made possible via the U.S. National Science Foundation Office of Polar Programs and their contract with Battelle Arctic Research Operations (contract #49100420C0001). Ny Ålesund, Scoresbysund and Sodankylä ozonesonde data are obtained as part of the Network for the Detection of Atmospheric

Composition Change (NDACC). Data is available via https://ndacc.larc.nasa.gov/index.php/stations. Click on the relevant site location to access the data files. Ozonesonde data for Alert, Resolute and Eureka have been reprocessed according to Tarasick et al. (2016), available at https://hegiftom.meteo.be/datasets/ozonesondes.

All model output files in NetCDF format from the simulations used in this study can be found here: https://open.canada.ca/data/en/dataset/c9a333ea-b81c-4df3-9880-ea7c3daeb76f. Model codes for GISS-E2.1 are available at: https://www.giss.nasa.gov/tools/modelE/.

Open-source codes for the Mann-Kendall test associated with Sen's slope are distributed under the BSD 3-Clause License in dedicated GitHub repositories hosted within the "mannkendall" organization (https://github.com/mannkendall), a Matlab (Collaud Coen and Vogt, 2020, https://doi.org/10.5281/zenodo.4134618, https://github.com/mannkendall/Matlab), Python (Vogt, 2020, https://doi.org/10.5281/zenodo.4134435, https://github.com/mannkendall/Python), and R (Bigi and Vogt, 2020, https://doi.org/10.5281/zenodo.4134632, https://github.com/mannkendall/R). Last access for all codes 27 January 2023.

References

AMAP. (2015). AMAP Assessment 2015: Black carbon and ozone as Arctic climate forcers. *Arctic Monitoring and Assessment Programme (AMAP)*, 116, ISBN 978-82-7971-092-9. https://www.amap.no/documents/doc/amap-assessment-2015-black-carbon-and-ozone-as-arctic-climate-forcers/1299

AMAP (2021). AMAP Assessment 2021: Impacts of short-lived climate forcers on Arctic climate, air quality, and human health. Arctic Monitoring and Assessment Programme (AMAP), Tromsø, Norway, in press, 2023. Last access 24 January 2023. https://www.amap.no/documents/doc/amap-assessment-2021-impacts-of-short-lived-climate-forcers-on-arctic-climate-air-quality-and-human-health/3614

Andersson, C., Alpfjord, H., Robertson, L., Karlsson, P. E., & Engardt, M. (2017) Reanalysis of and attribution to near-surface ozone concentrations in Sweden during 1990–2013, *Atmospheric Chemistry and Physics, 17*, 13869–13890, https://doi.org/10.5194/acp-17-13869-2017.

Anenberg, S. C., Horowitz, L. W., Tong, D. Q., & West, J. J. (2010). An estimate of the global burden of anthropogenic ozone and fine particulate matter on premature human mortality using atmospheric modeling. *Environmental Health Perspectives*, *118*(9), 1189–1195. https://doi.org/10.1289/ehp.0901220

371 Arnold, S. R., Lombardozzi, D., Lamarque, J.-F., Richardson, T., Emmons, L. K., Tilmes, S., et al.
372 (2018). Simulated global climate response to tropospheric ozone-induced changes in plant
373 transpiration. *Geophysical Research Letters*, *45*(23), 13070–13079.
374 https://doi.org/10.1029/2018GL079938

375 Bahramvash Shams, S., Walden, V. P., Petropavlovskikh, I., Tarasick, D., Kivi, R., Oltmans, et al. (2019)
376 Variations in the vertical profile of ozone at four high-latitude Arctic sites from 2005 to 2017,
377 *Atmospheric Chemistry and Physics, 19*, 9733–9751, https://doi.org/10.5194/acp-19-9733-2019

378 Barrie, L., Bottenheim, J., Schnell, R. et al. (1988) Ozone destruction and photochemical reactions at
379 polar sunrise in the lower Arctic atmosphere. *Nature, 334***,** 138–141.
380 https://doi.org/10.1038/334138a0

381 Benavent, N., Mahajan, A. S., Li, Q., Cuevas, C. A., Schmale, J., Angot, H., et al. (2022). Substantial
382 contribution of iodine to Arctic ozone destruction. *Nature Geoscience*, 15(10), 770–773.
383 https://doi.org/10.1038/s41561-022-01018-w

384 Bougoudis, I., Blechschmidt, A.-M., Richter, A., Seo, S., Burrows, J. P., Theys, N., & Rinke, A. (2020).
385 Long-term time series of Arctic tropospheric BrO derived from UV–VIS satellite remote sensing and
386 its relation to first-year sea ice. *Atmospheric Chemistry and Physics*, 20(20), 11869–11892.
387 https://doi.org/10.5194/acp-20-11869-2020

388 Bowman, H., Turnock, S., Bauer, S. E., Tsigaridis, K., Deushi, M., Oshima, N., et al. (2022). Changes in
389 anthropogenic precursor emissions drive shifts in the ozone seasonal cycle throughout the northern
390 midlatitude troposphere. *Atmospheric Chemistry and Physics*, 22(5), 3507–3524.
391 https://doi.org/10.5194/acp-22-3507-2022

392 Christiansen, A., Mickley, L. J., Liu, J., Oman, L. D., & Hu, L. (2022). Multidecadal increases in global
393 tropospheric ozone derived from ozonesonde and surface site observations: can models reproduce
394 ozone trends? *Atmospheric Chemistry and Physics*, 22(22), 14751–14782.
395 https://doi.org/10.5194/acp-22-14751-2022

396 Christiansen, B., Jepsen, N., Kivi, R., Hansen, G., Larsen, N., and Korsholm, U. S. (2017) Trends and
397 annual cycles in soundings of Arctic tropospheric ozone, *Atmospheric Chemistry and Physics,* 17,
398 9347–9364. https://doi.org/10.5194/acp-17-9347-2017

399 Clifton, O. E., Fiore, A. M., Massman, W. J., Baublitz, C. B., Coyle, M., Emberson, L., et al. (2020). Dry
400 deposition of ozone over land: Processes, measurement, and modeling. *Reviews of Geophysics*,
401 *58*(1). https://doi.org/e2019RG000670

402 Collaud Coen, M., Andrews, E., Bigi, A., Martucci, G., Romanens, G., Vogt, F. P. A., and Vuilleumier,
403 L. (2020) Effects of the prewhitening method, the time granularity, and the time segmentation on the
404 Mann–Kendall trend detection and the associated Sen's slope, *Atmospheric Measurement*
405 *Techniques, 13*, 6945-6964. https://doi/org/10.5194/amt-13-6945-2020

406 Cooper, O. R., Schultz, M. G., Schröder, S., Chang, K.-L., Gaudel, A., Benítez, G. C., et al. (2020).
407 Multi-decadal surface ozone trends at globally distributed remote locations. *Elementa: Science of the*
408 *Anthropocene*, *8*, 23. https://doi.org/10.1525/elementa.420

409 Dibb, J. E. (2007). Vertical mixing above Summit, Greenland: Insights into seasonal and high frequency
410 variability from the radionuclide tracers 7Be and 210Pb. *Atmospheric Environment*, 41(24), 5020–
411 5030. https://doi.org/10.1016/j.atmosenv.2006.12.005

412 Fiore, A. M., Hancock, S. E., Lamarque, J.-F., Correa, G. P., Chang, K.-L., Ru, M., et al. (2022).
413 Understanding recent tropospheric ozone trends in the context of large internal variability: a new
414 perspective from chemistry-climate model ensembles. *Environmental Research: Climate*, 1(2),
415 025008. https://doi.org/10.1088/2752-5295/ac9cc2

416 Gaudel, A., Cooper, O. R., Ancellet, G., Barret, B., Boynard, A., Burrows, J. P., et al. (2018).
417 Tropospheric Ozone Assessment Report: Present-day distribution and trends of tropospheric ozone
418 relevant to climate and global atmospheric chemistry model evaluation. *Elementa: Science of the*
419 *Anthropocene*, *6*, 39. https://doi.org/10.1525/elementa.291

420 Griffiths, P. T., Murray, L. T., Zeng, G., Shin, Y. M., Abraham, N. L., Archibald, A. T., et al. (2021).
421 Tropospheric ozone in CMIP6 simulations. *Atmospheric Chemistry and Physics, 21(5),* 4187–4218.
422 https://doi.org/10.5194/acp-21-4187-2021

423 Gunsch, M. J., Kirpes, R. M., Kolesar, K. R., Barrett, T. E., China, S., Sheesley, R. J., et al. (2017).
424 Contributions of transported Prudhoe Bay oil field emissions to the aerosol population in Utqiaġvik,
425 Alaska. *Atmospheric Chemistry and Physics, 17(17)*, 10879–10892. https://doi.org/10.5194/acp-17-
426 10879-2017

427 Hirdman, D., Sodemann, H., Eckhardt, S., Burkhart, J. F., Jefferson, A., Mefford, T., et al. (2010). Source
428 identification of short-lived air pollutants in the Arctic using statistical analysis of measurement data
429 and particle dispersion model output. *Atmospheric Chemistry and Physics*, 10(2), 669–693.
430 https://doi.org/10.5194/acp-10-669-2010

431 Jhun, I., Coull, B. A., Zanobetti, A., & Koutrakis, P. (2015). The impact of nitrogen oxides concentration
432 decreases on ozone trends in the USA. *Air Quality, Atmosphere and Health*, 8(3), 283–292.
433 https://doi.org/10.1007/s11869-014-0279-2

434 Koo, J. H., Wang, Y., Kurosu, T. P., Chance, K., Rozanov, A., Richter, A., et al. (2012) Characteristics of
435 tropospheric ozone depletion events in the Arctic spring: analysis of the ARCTAS, ARCPAC, and
436 ARCIONS measurements and satellite BrO observations. *Atmospheric Chemistry and Physics*,
437 12(20), 9909–9922. https://doi.org/10.5194/acp-12-9909-2012

438 Law, K. S., Stohl, A., Quinn, P. K., Brock, C. A., Burkhart, J. F., Paris, J.-D., et al. (2014). Arctic air
439 pollution: New insights from POLARCAT-IPY. *Bulletin of the American Meteorological Society*,
440 95(12), 1873–1895. https://doi.org/10.1175/bams-d-13-00017.1

441 Liu, J., Rodriguez, J. M., Oman, L. D., Douglass, A. R., Olsen, M. A., & Hu, L. (2020). Stratospheric
442 impact on the Northern Hemisphere winter and spring ozone interannual variability in the
443 troposphere. *Atmospheric Chemistry and Physics*, *20*(11), 6417–6433. https://doi.org/10.5194/acp-
444 20-6417-2020

445 Mudryk, L., Santolaria-Otín, M., Krinner, G., Ménégoz, M., Derksen, C., Brutel-Vuilmet, C., et al.
446 (2020). Historical Northern Hemisphere snow cover trends and projected changes in the CMIP6
447 multi-model ensemble. *The Cryosphere*, 14(7), 2495–2514. https://doi.org/10.5194/tc-14-2495-2020

448 Oltmans, S. J., Johnson, B. J., & Harris, J. M. (2012) Springtime boundary layer ozone depletion at
449 Barrow, Alaska: Meteorological influence, year-to-year variation, and long-term change, *Journal of*
450 *Geophysical Research,* 117, D00R18, https://doi.org/10.1029/2011JD016889

451 Rap, A., Richards, N. A. D., Forster, P. M., Monks, S. A., Arnold, S. R., and Chipperfield, M. P. (2015).
452 Satellite constraint on the tropospheric ozone radiative effect. *Geophysical Research Letters*, *42*(12),
453 5074–5081. https://doi.org/10.1002/2015GL064037

454 Sand, M., Berntsen, T. K., von Salzen, K., Flanner, M. G., Langner, J., & Victor, D. G. (2016). Response
455 of Arctic temperature to changes in emissions of short-lived climate forcers. *Nature Climate*
456 *Change*, 6(3), 286–289. https://doi.org/10.1038/nclimate2880

457 Schmale, J., Arnold, S. R., Law, K. S., Thorp, T., Anenberg, S., Simpson, W. R., Mao, J., and Pratt, K. A.
458 (2018) Local Arctic air pollution: A neglected but serious problem, *Earth's Future*, 6, 1385-1412.
459 https://doi.org/10.1029/2018ef000952

460 Schmeisser, L., Backman, J., Ogren, J. A., Andrews, E., Asmi, E., Starkweather, S., et al. (2018).
461 Seasonality of aerosol optical properties in the Arctic. *Atmospheric Chemistry and Physics*, 18(16),
462 11599–11622. https://doi.org/10.5194/acp-18-11599-2018

463 Sen, P. K. (1968), Estimates of the regression coefficient based on Kendall's Tau, *Journal of the*
464 *American Statistical Association, 63*, 1379-1389. https://doi.org/10.1080/01621459.1968.10480934

465 Sharma, S., L. A. Barrie, E. Magnusson, G. Brattstrom, W. R. Leaitch, A. Steffen and S. Landsberger
466 (2019) A factor and trends analysis of multidecadal lower tropospheric observations of Arctic
467 Aerosol Composition, Black Carbon, Ozone, and Mercury at Alert, Canada. *Journal of Geophysical*
468 *Research-Atmospheres, 124*(24): 14133-14161. https://doi.org/10.1029/2019JD030844

469 Simpson, W. R., von Glasow, R., Riedel, K., Anderson, P., Ariya, P., Bottenheim, J., et al. (2007).
470 Halogens and their role in polar boundary-layer ozone depletion. *Atmospheric Chemistry and*
471 *Physics*, *7*(16), 4375–4418. https://doi.org/10.5194/acp-7-4375-2007

472 Tarasick, D. W., Davies, J., Smit, H. G. J., & Oltmans, S. J. (2016). A re-evaluated Canadian ozonesonde
473 record: measurements of the vertical distribution of ozone over Canada from 1966 to 2013.
474 *Atmospheric Measurement Techniques*, *9*(1), 195–214. https://doi.org/10.5194/amt-9-195-2016

475 Tarasick, D., Galbally, I.E., Cooper, O.R., Schultz, M.G., Ancellet, G., Leblanc, et al. (2019).
476 Tropospheric Ozone Assessment Report: Tropospheric ozone from 1877 to 2016, observed levels,

trends and uncertainties. *Elementa: Science of the Anthropocene, 7*: 39. https://doi.org/10.1525/elementa.376

Theil, H. (1950) A rank-invariant method of linear and polynomial regression analysis, *Nederl. Akad. Wetensch., Proc., 53*, 386--392, https://ir.cwi.nl/pub/18446

Turnock, S. T., Allen, R. J., Andrews, M., Bauer, S. E., Deushi, M., Emmons, L., et al. (2020). Historical and future changes in air pollutants from CMIP6 models. *Atmospheric Chemistry and Physics*, 20(23), 14547–14579. https://doi.org/10.5194/acp-20-14547-2020

von Salzen, K., Whaley, C. H., Anenberg, S. C., Van Dingenen, R., Klimont, Z., Flanner, M. G., et al. (2022). Clean air policies are key for successfully mitigating Arctic warming. *Communications Earth & Environment*, 3(1), 222. https://doi.org/10.1038/s43247-022-00555-x

Wang, H., X. Lu, D. J. Jacob, O. R. Cooper, K.-L. Chang, K. Li, et al. (2022a) Global tropospheric ozone trends, attributions, and radiative impacts in 1995-2017: an integrated analysis using aircraft (IAGOS) observations, ozonesonde, and multi-decadal chemical model simulations, *Atmospheric Chemistry and Physics*, *22,* 13753-13782. https://doi.org/10.5194/acp-22-13753-2022

Wang, T, L. Xue, Z. Feng, J. Dai, Y. Zhang, & Y. Tan (2022b) *Environmental Research Letters,* 17**,** 063003, Ground-level ozone pollution in China: a synthesis of recent findings on influencing factors and impacts. https://doi.org/10.1088/1748-9326/ac69fe

Whaley, C. H., Mahmood, R., von Salzen, K., Winter, B., Eckhardt, S., Arnold, et al. (2022), Model evaluation of short-lived climate forcers for the Arctic Monitoring and Assessment Programme: a multi-species, multi-model study, *Atmospheric Chemistry and Physics, 22*, 5775–5828. https://doi.org/10.5194/acp-22-5775-2022

Whaley, C. H., Law, K. S., Hjorth, J. L., Skov, H., Arnold, S. R., Langner, J., Pernov, et al. (2023), Arctic tropospheric ozone: assessment of current knowledge and model performance. *Atmospheric Chemistry and Physics*, 23, 637-661. https://doi.org/10.5194/acp-23-637-2023

Young, P.J., V. Naik, A. M. Fiore, A. Gaudel, J. Guo‖, M. Y. Lin, et al. (2018) Tropospheric Ozone Assessment Report: Assessment of global-scale model performance for global and regional ozone distributions, variability, and trends. *Elementa: Science of the Anthropocene*, 6: 10. https://doi.org/10.1525/elementa.265

Zeng, G., Morgenstern, O., Williams, J. H. T., O'Connor, F. M., Griffiths, P. T., Keeble, J., et al. (2022). Attribution of stratospheric and tropospheric ozone changes between 1850 and 2014 in CMIP6 models. *Journal of Geophysical Research: Atmospheres*, 127. https://doi.org/10.1029/2022JD036452

Zhang, J., F. Xie, W. Tian, Y. Han, K. Zhang, Y. Qi et al. (2017) Influence of the Arctic Oscillation on the vertical distribution of wintertime ozone in the stratosphere and upper troposphere over the Northern Hemisphere, *Journal of Climate*, 30(8). https://doi.org/10.1175/JCLI-D-16-0651.1